PAPER • **OPEN ACCESS**

The Effect of Boron Addition on The Microstructure and Corrosion Resistance of Cu-Al-Ni Shape-Memory Alloys Prepared by Powder Technology

To cite this article: Abdulraheem Kadhim Abid Ali and Nawal Mohammed Dawood 2020 *IOP Conf. Ser.: Mater. Sci. Eng.* **987** 012028

The Effect of Boron Addition on The Microstructure and Corrosion Resistance of Cu-Al-Ni Shape-Memory Alloys Prepared by Powder Technology

ABDULRAHEEM KADHIM ABID ALI[1], NAWAL MOHAMMED DAWOOD[1*]
[1] Department of Metallurgical Engineering, College of Materials Engineering, Babylon University, Babylon, Iraq
[*]Corresponding author: mat.newal.mohammed@uobabylon.edu.iq

Abstract. Due to their promising mechanical characteristics, copper-based shape-memory alloys (SMAs) are crucial for numerous applications. This research inspects the outcomes of various quantities (0.4%, 0.8% and 1.2% wt) of boron (B) additions on the resistance against corrosion and the microstructure of Cu-Al-Ni SMAs using SEM, EDS, XRD and electrochemical tests in a solution of 3.5% NaCl. Numerous measurement baths were used for aged / unaged Cu-Al-Ni-xB SMAs. The electrochemical tests were performed over several periods to confirm the reliability of the corrosion-resistance property, after which the samples were verified using solutions of 3.5% NaCl. The experimental results demonstrated that adding 1.2% wt B followed by an ageing process resulted in an improvement in the corrosion resistance in Cu-Al-Ni SMAs and a decrease in the corrosion rate by 58%.
Keywords: *Cu-Al-Ni alloys; powder metallurgy; electrochemical test; SMA; microstructures.*

1. Introduction

Since the beginning of this century, shape-memory alloys (SMAs) have been considered smart materials with applications that vary from medicine to military, and Cu-based SMAs are extensively in demand as a result of their low cost and useful mechanical and shape-memory properties. Cu-based alloys are an appropriate auxiliary for nickel-titanium (Ni-Ti) alloys in engineering projects, such as buildings, fasteners, bridge-damping elements, oil wells and actuators' requests. Their low cost, simple manufacturing and wide range of temperatures [1] provide additional support. They have a sufficient recovery strain from two per cent to four per cent and a wide variety in temperature transformations (from 100°C to 170°C) [2].

However, when these materials are used in a corrosion-erosion environment, the damage must be considered, particularly in extremely corrosive surroundings, such as oil rigs and coastal fields. Furthermore, SMA systems are widely applicable and simple to use; for example, a portion of the components are an entire system by themselves. Moreover, this property may present galvanic corrosions because SMAs directly interact with other kinds of metals. One of the reasons why SMAs are useful in

manufacturing plants is because the Cu-Al-Ni alloy has a strong resistance against corrosion since the formed alumina deposit functions as an inert layer [3].
However, it must be noted that the Cu-Al-Ni alloys become weak post-ageing, which leads to changes in its mechanical behaviour. Once it is exposed to high temperatures, its duration of operation increases [4]. Similarly, more studies have been conducted on Cu-Al-Ni's characteristics in relation to its application ranges than on its extensive demand in industries. There are numerous methods to improve the characteristics of SMAs; one such method is grain fine-tuning and adding minor amounts of the four elements, such as titanium and zirconium, to the SMAs [5, 6].

The Cu-Al-Ni SMAs corrosion resistance increases; for instance, the grains become finer owing to elements, such as manganese and titanium [6, 7]. However, adding cobalt to Cu-Al-Ni can increase both the alloys' mechanical properties and its temperature in the austenitic phases. This means that this combination can be employed at higher temperatures [8].
Although the Cu-Al-Ni alloy has a relatively strong corrosion resistance and mechanical properties, it was less striking in comparison to the extensively utilised NiTi, which has restricted use. However, even though it is used in environments with high corrosion, further studies on the corrosive behaviours of the Cu-Al-Ni SMAs alloy in specific surroundings are required.

Abid Ali et al. [9] measured the effects of iron addition on the corrosive resistance of Cu-Al-Ni SMA using five per cent NaOH and iron (0.4%, 0.8% and 1.2% wt). The outcomes show that the Cu-Al-Ni SMAs have a lower corrosion rate in the austenitic phase compared to the martensitic phase. It was also found that a stronger corrosion resistance was attained by adding 0.4% Fe. Furthermore, Abid and Al-Tai [10] measured the effects of adding silicon (0.4%, 0.8% and 1.2% wt) on the corrosion resistance and dry sliding wear of Cu-Al-Ni SMAs in 3.5% concentration of NaCl. Their results demonstrated that Cu-Al-Ni SMAs have a lower corrosion rate in the austenitic phase compared to the martensitic phase. Gojic et al. [11] verified the microstructures and electro-chemical property of Cu-Al-Ni SMAs on the corrosion resistance of Cu-Al-Ni SMAs in a 0.5 ml NaCl solution, which was examined by linear and open-circuit potential tests. The results showed that the adsorption of chloride ion on the electrode exterior results in a decrease in the EOCP values and the failure of the defensive external oxide scale. Furthermore, Saud et al. [12] examined the effects of tantalum (Ta) on the corrosion resistance, microstructures, damping and shape-memory behaviour of pre-alloyed Cu-Al-Ni SMAs. Polarisation examinations in 3.5% NaCl solutions showed that the corrosion resistance increased with Ta concentrations and created a strong inert layer.
This research aims to evaluate the corrosion resistance and microstructures of Cu-Al-Ni SMAs with boron (B) additions (0.4%, 0.8% and 1.2% wt) in a 3.5% sodium chloride solution. This was done via powder metallurgy.

2. Experimental Procedures

2.1. Sample Preparation

The samples were shaped using the powder technology with the essential powders Cu, Al, Ni and B. Table 1 demonstrates the size of the particles, as well as the purities and compositions of the used powders. The powders were mixed in a planetary ball mill for approximately six hours with a mixing ratio of 1:5 at a weight and rotation speed of 350 rpm. Exactly 0.5 cc ethyl alcohol was used to minimise the temperature that was generated by friction between the balls with walls and powder. After mixing, the wet mixtures were left to dry at room temperature for approximately 30 minutes. After that, they were placed in polyethylene zip locked bags. Later, the mixed powder was pressed in a hydraulic press at 800 MPa using cylindrical stainless-steel die of ten mm diameter. Then, the green specimens were put in a furnace with a vacuum for approximately two hours at 550 ˚C and were continued to be sintered at 950 ˚C for about 180 min with the heating rate as ten ℃ / min for both the sintering stages. The samples were then cooled under

the vacuum until they reached room temperature. Next, the sintered samples were heat-treated at 850 °C for 60 minutes and dipped in iced water. Following that, the samples were heated to 300 °C for 1800 min and immersed in water to age the intermetallic compound (γ_2) and steady the martensite phase.

2.2. Preparation of the Samples for Microstructure Observation

The samples were then wet-grinded by 180, 400, 800, 1,000, 1,200, 1,500, 2,000, 2,500 and 3,000 grits SiC papers using a grinding wheel and were later polished with papers and diamonds with a one μm to three μm particle size. All samples were then washed using distilled water and dried in warm air. Later, the samples were treated with an etching solution (2.5 g $FeCl_3$ $6H_2O$ + 48 ml CH_3OH + ten ml HCl) and ferric chloride acid / methanol / hydrochloric acid [13] for ten seconds. They were then used for SEM and EDS tests.

Table 1. Elementals powder specification with compositions.

Properties	Copper	Aluminium	Nickel	Boron
Particle size (μm)	14	15	27	8
Purity (%)	99.95	99.92	99.95	99.94
Prepared	83	13	4	…..
samples	82.6	13	4	0.4
composition	82.6	13	4	0.8
(wt %)	81.8	13	4	1.2

2.3. Material Characterisation

A sample with dimensions of (d = ten mm, t = five mm) was prepared for XRD characteristics using Mini flex2. X-rays with CuKα radiations at 30 mA and 40 Kv were performed. The device's scanning speed was two° / minute with an angle of 2θ, ranging from 30° to 90° with step 0.02° / sec.

2.4. Electro-Chemical Test

The corrosion performance of Cu-Al-Ni SMAs with and without (0.4%, 0.8% and 1.2% wt) the addition of B was achieved at 25 °C in the air in a beaker with 350 ml of 3.5% NaCl (3.5 gm NaCl + 96.5 ml distilled water). The corrosion performance of the alloys was examined using the Tafel potentiostat method WENKING M lap to measure the corrosion current and corrosion potential.

Three electrodes were used for the potentiodynamic polarisation test. A platinum wire was measured for the counter electrodes and reference electrodes for saturated calomel electrodes (SCE) while the sample was the working electrode. The polarisation curves were measured potentiostatically at a scanning rate of 0.35 mVs^{-1}. For all measurements, the electrodes were maintained at the open circuit for at least ten–20 minutes for stabilisation, and then the Eo was obtained. The electrochemical system that was used is shown in Figure 1.

Fig 1. The electrochemical system.

3. Results and Discussions

3.1. Microstructures and X-ray Diffractions for Phase Analysis.

The microstructure and EDS examination of the homogenising Cu-Al-Ni SMA samples with and without alterations after ageing treatments are illustrated in Figures 2–6. The results showed the following two different phases: needle-like for ß$_1$′ and plate-like for γ_1′. These two phases were also mentioned in numerous additional revisions [4, 8, 14 & 15]. Like other metallic materials and alloys, the Cu-Al-Ni SMAs grain sizes increased with an increase in the ageing treatments. It was observed that the width of the plates increased, whereas the needles reduced after ageing. Furthermore, the microstructure showed that the grain size of the Cu-Al-Ni-xB SMAs was the finest in the case of increased B content; on the other hand, a different phase, in the formula of precipitates, shaped the matrices. Saud et al. [8] identified the phase as the γ_2 phase as an intermetallic compound. These precipitates tend to isolate the grains' boundaries lengthways, as shown in Figure 1d, and augmented in extent with higher B gratified. This conclusion was also corroborated by an EDX analysis, as shown in Figures 2–6, wherein a higher content of B (1.2% wt) was found in the precipitate. Figure 7 illustrates the XRD results of the aged Cu-Al-Ni SMAs, in which α Cu and intermetallic compounds $AlCu_3$ were found. The other phases that were formed between the elements present in the alloy that play an important role in improving the corrosion resistance of the alloy did not appear in the X-ray diffraction due to their occurrence outside the limits of X-ray detection.

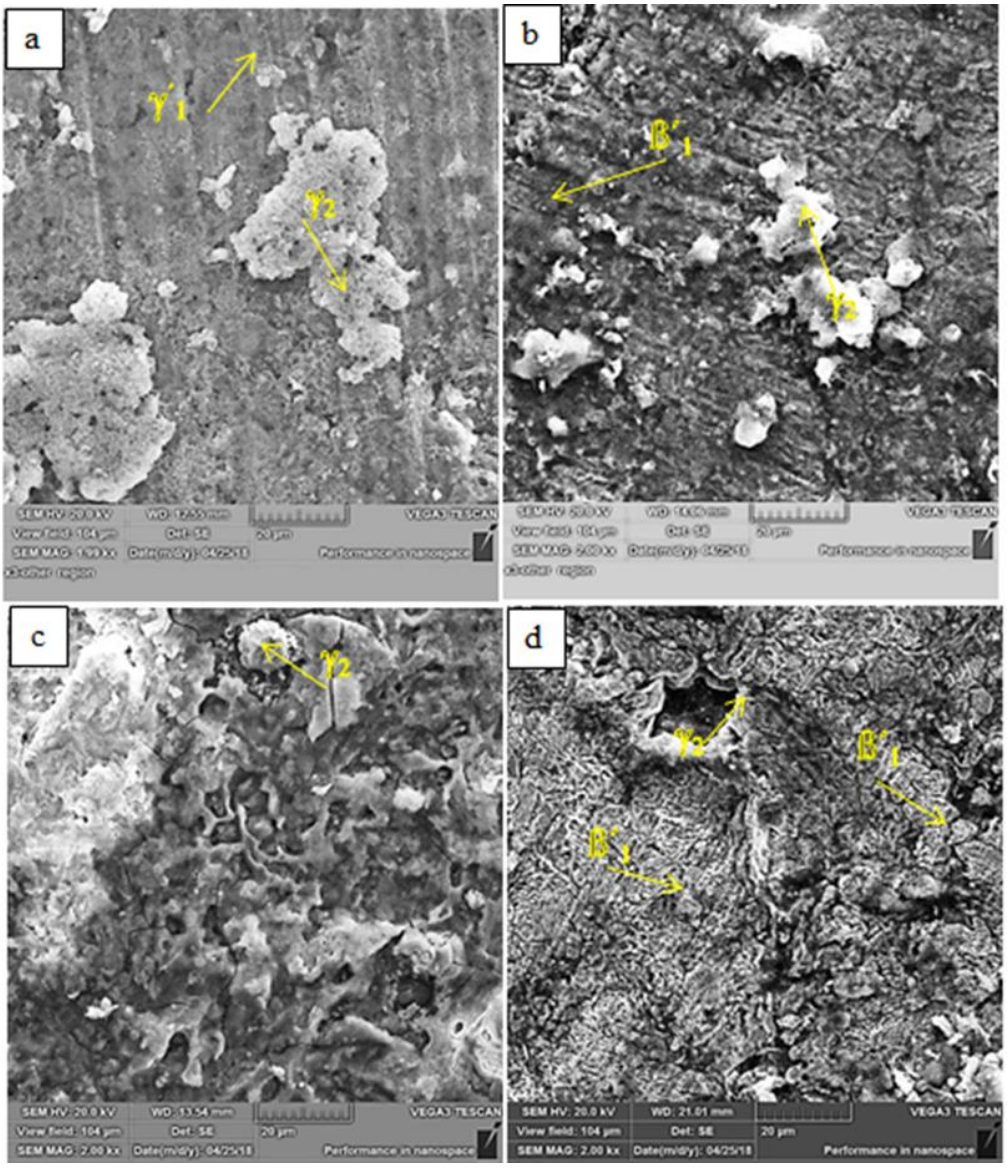

Fig 2. SEM microstructure of (a) Cu-Al-Ni SMAs; (b) Cu-Al-Ni 0.4% B SMAs; (c) Cu-Al-Ni 0.8% B SMAs; and (d) Cu-Al-Ni 12%B SMAs.

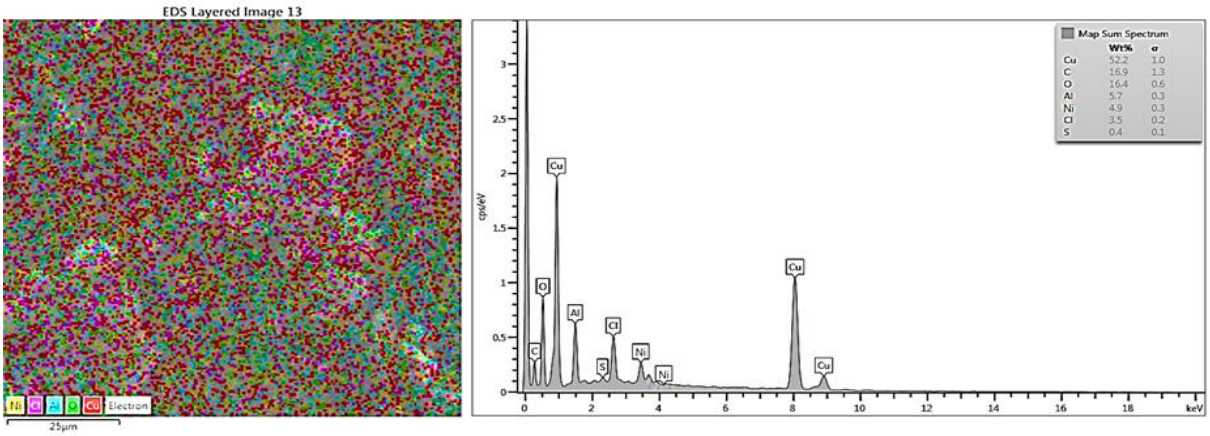

Fig 3. The EDX analysis of Cu-Al-Ni SMAs.

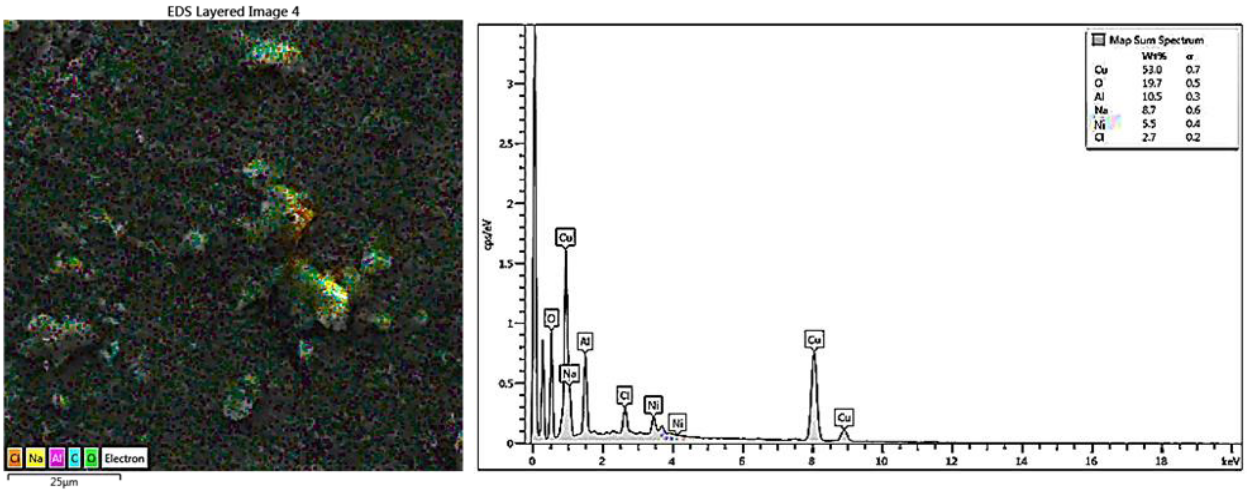

Fig 4. The EDX analysis of Cu-Al-Ni 0.4 B SMAs.

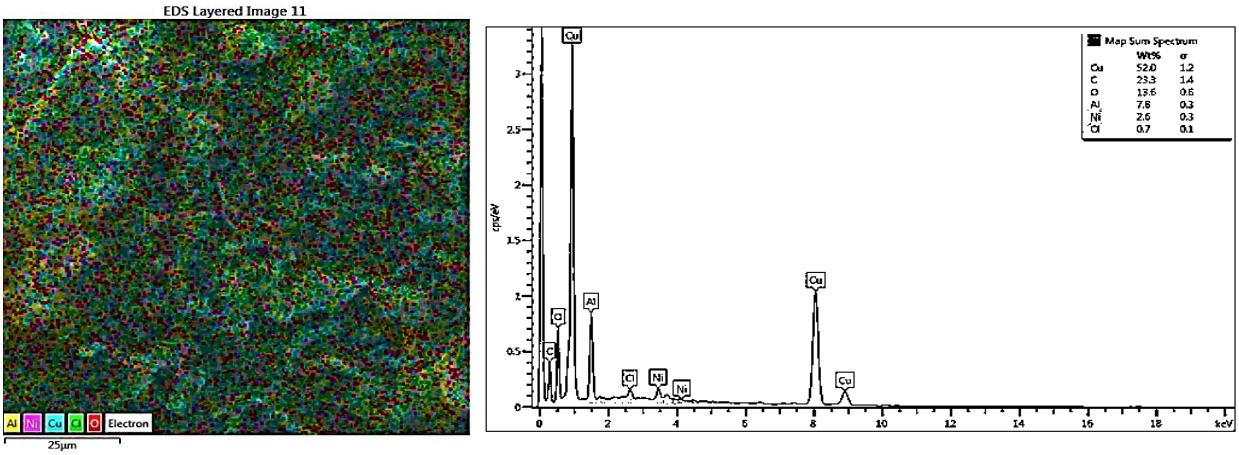

Fig 5. The EDX analysis of Cu-Al-Ni 0.8 B.

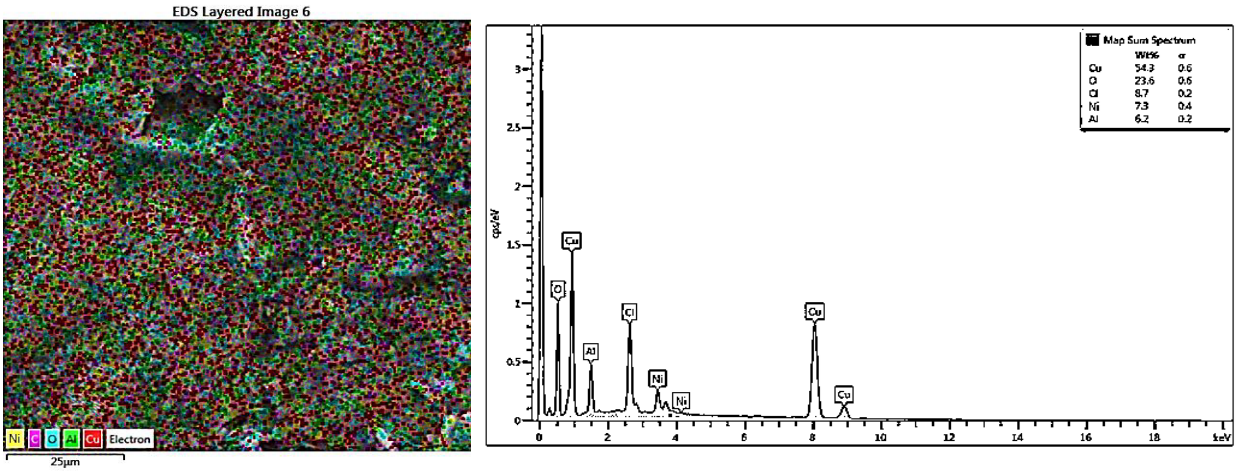

Fig 6. The EDX analysis of Cu-Al-Ni 1.2 B SMAs.

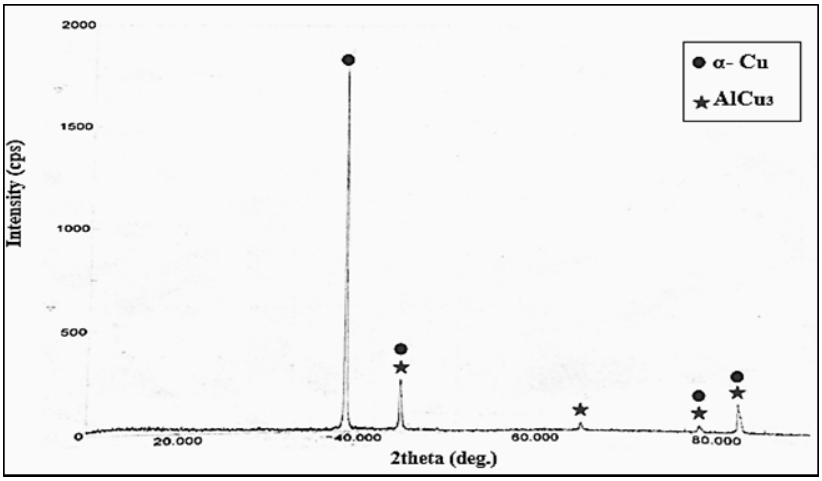

Fig 7. The XRD test results of Cu-Al-Ni SMAs.

3.2 Electrochemical Test Result

Figure 8 shows the polarisation diagrams of Cu-Al-Ni SMAs with and without (0.4%, 0.8% and 1.2% wt) the addition of B. The Cu-Al-Ni SMAs' reduction in anodic polarisation tendency and refinement in the cathodic polarisation performance was also seen [16]. It was observed that the existence of B in the passivation surface improved the resistance of the alloy from chlorine ion in the sodium chloride solution better than in the absence of B [17]. The corrosion rate (mpy), corrosion potential (E_{corr}) and corrosion current density (I_{corr}) of the samples were determined from the polarisation's curves, as shown in Table 2.

Table 2. Polarisation parameters of Cu-Al-Ni SMAs in 3.5% NaCl solution before and after B additions.

Alloys composition	**Corrosion potential E_{corr} (mV)**	**Current density I_{corr} (µA / cm^2)**	**Corrosion rate (mpy)**
Cu-Al-Ni	-306	34.6	14.95
Cu-Al-Ni-0.4% B	-596	21.3	9.063
Cu-Al-Ni-0.8% B	-431.4	8.5	3.56
Cu-Al-Ni 1.2% B	-446.8	5.5	2.27

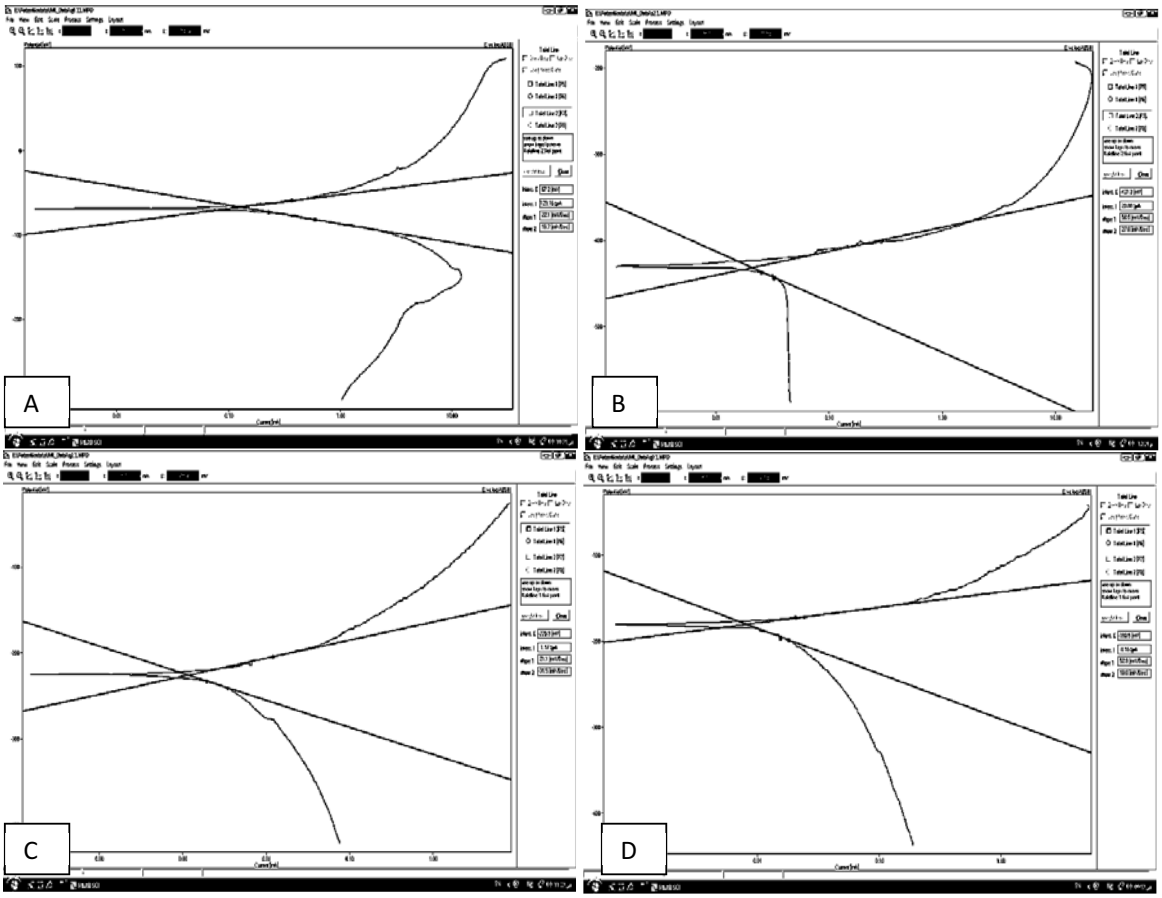

Fig 8. (A) the polarisation of Cu-Al-Ni SMAs; (B) the polarisation of Cu-Al-Ni 0.4%B SMAs; (C) the polarisation of Cu-Al-Ni 0.8%B SMAs; and (D) the polarisation of Cu-Al-Ni 1.2%B S.

I_{corr} is associated with mpy, as shown in the following empirical equation [18, 19]:

$$C.R\ (mpy) = \frac{0.13 \times I_{corr} \times E.W}{A \times \rho} \ldots\ldots \text{Eq1}$$

Where A = area of the surface (cm^2).
ρ = density of the sample (g / cm^2).
I_{corr} = corrosion current density ($\mu A / cm^2$).
E.w = equivalent weight.
As shown in Table 2, the corrosion rate of the Cu-Al-Ni SMA is 14.95 mpy. After adding B (0.4%, 0.8% and 1.2% wt), the rate became 9.063, 3.56 and 2.27 mpy, respectively. The creation of corrosion products Al_2O_3 after the corrosion tests in 3.5% NaCl is the cause of the decrease in the corrosion rate from 14.95 mpy in Cu-Al-Ni SMA to 2.27 mpy in Cu-Al-Ni 1.2% B SMA. For the higher effects, the corrosion penetration rate was lower than approximately 20 mpy, which was satisfactory [20, 21].

4. Conclusion

Sintering samples at 550 °C for 120 minutes and 950 °C for 180 minutes (with and without 0.4%, 0.8% and 1.2% wt B) was an efficient method of preparing Cu-Al-Ni alloy structures. The sintered samples were heated at 850 °C for 60 minutes, rapidly immersed in iced water, heated to 300 °C for 1800 minutes and put in water again to age the intermetallic compound (γ_2) and stabilise the martensite phase. The ageing of Cu-Al-Ni SMAs was enough to get γ′ (coarse, martensite plate-like) and ß′ (needle-like shape), whereas the B addition to Cu-Al-Ni SMA tended to refine γ′ (coarse martensite plate-like). The electrochemical test displayed that the corrosion rate decreased from 14.95 mpy to 2.27 mpy when 1.2% wt B was added. Therefore, we conclude that an increase in boron leads to an improvement in the resistance of Cu-Al-Ni SMAs against corrosion.

5. References

[1] C. L'excellent, 2013 "Shape Memory Alloy Handbook" John Wiley and Son, New York, USA.
[2] D. Lagudas, 2006 "Shape Memory Alloy: Engineering Modeling" Springer, Berlin, Germany.
[3] A. Schüssler, H. Exner, 1993, The corrosion of nickel-aluminium bronzes in seawater—I. Protective layers formation and the passivation mechanism. Corros Sci, .34(11):1793–1802.
[4] N. Suresh, U. Ramamurty, 2008, Ageing response and its effect on the functional properties of Cu-Al-Ni shape memory alloys. J Alloys Compds, 449(1–2):113–118.
[5] J.S. Lee, C. M. Wayman, 1986, Grain refinement of a Cu-Al-Ni shape memory alloy by Ti and Zr additions. Trans Japan Inst Met , 27(8):584–591.
[6] S. Saud, E. Hamzah, T. Abubakar, M. Zamri, M. Tanemura, 2014, Influence of Ti additions on the martensitic phase transformation and mechanical properties of Cu-Al-Ni shape memory alloys. J Therm Anal Calorim, 1:111–122,
[7] S. Saud, E. Hamzah, T. Abubakar, HR. Bakhsheshi-Rad, M. Zamri, M. Tanemura, 2014, Effects of Mn additions on the structure, mechanical properties, and corrosion behavior of Cu-Al-Ni shape memory alloys. J Mater Eng Perform , 11:3620–3629.
[8] S. Saud, E. Hamzah, T. Abubakar, HR. Bakhsheshi-Rad, 2015, Thermal aging behavior in Cu-Al-Ni-xCo shape memory alloys. J Therm Anal Calorim , 119(2):1273–1284.

[9] Abdul-Raheem K. AbidAli, and Z. T. K. Al-Tai, 2012, The effect of silicon addition on the dry sliding wear and corrosion behavior of Cu Al Ni shape memory alloy. The Iraqi Journal for Mechanical And Material Engineering, 12(1).

[10] Abdul-Raheem K. AbidAli, and Z. T. K. Al-Tai, 2010 , The effect of iron addition on the dry sliding wear and corrosion behavior of Cu Al Ni shape memory alloy, adopted from Journal of Eng. & Tech, 28(24).

[11] M. Gojic, L. Vrsalovi, S. Kozuh, A. Kneissl, I. Anzel, S. Gudi, B. Kosec, and M. Kliski, 2011, Electrochemical and microstructural study of Cu-Al-Ni shape memory alloy, adopted from The Journal of Alloys and Compounds: 9782–9790.

[12] Safaa N. Saud, E. Hamzah, H.R. Bakhsheshi-Rad, and T.Abubakar. 2017 ,Effect of Ta Additions on the Microstructure, Damping, and Shape Memory Behaviour of Prealloyed Cu-Al-Ni Shape Memory Alloys, adopted from Hindawi Publishing Corporation, Volume1 , Article ID 1789454, 13 p46.

[13] S. Saud, E. Hamzah, H. Bakhsheshi-Rad, and T. Abubaker, 2014,Microstructure and corrosion behavior of Cu-Al- Ni shape memory alloys with Ag nanoparticles, Materials and Corrosion, 66(6).

[14] V. Recartea, RB Pérez-Sáeza, EH Bocanegrac, Nóc ML, and J. San Juan, ,2019, Dependence of the martensitic transformation characteristics on concentration in Cu-Al-Ni shape memory alloys. Mater Sci Eng A 273–275:380–384.

[15] H. Sakamoto, and KI. Shimizu, 1989, Effect of heat treatments on thermally formed martensite phases in mono crystalline Cu-Al-Ni shape memory alloy. ISIJ Int 29(5):395–404,.

[16] B. Chen, C. Liang, D. Fu, and D. Ren, 2005, Corrosion behavior of Cu and the Cu-Zn-Al shape memory alloy in simulated uterine fluid [J]. Contraception,72:221−224;79−89.

[17] E. N Kassab, L. Frotscher, M. Swaminathan, S. Maab, B. Rohweder, M. Gomes, and J G. Eggeler, 2014,Effect of ternary element addition on the corrosion behaviour of NiTi shape memory alloys [J]. Materials and Corrosion, 65:18−22.

[18] Annual Book of ASTM standards, (1988),Wear and erosion, Metal Corrosion, 3(2):G5–87.

[19] Alaa Abdulhasan Atiyah, Abdul-Raheem Kadhum, Abid Ali, Nawal Mohammed Dawood,2014, Characterization of NiTi and NiTiCu porous shape memory alloys prepared by powder metallurgy (Part I), Arabian Journal for Science and Engineering, 40(3):901–913.

[20] W.D. Callister, 2000, “Materials Science and Engineering”, 5th ed., United States of America.

[21] Alaa Abdulhasan Atiyah, Abdul-Raheem Kadhum Abid Ali, Nawal Mohammed Dawood, (2019) , Fabrication of porous NiTi shape memory alloy objects by powder metallurgy for biomedical applications, IOP Conf. Series: Materials Science and Engineer 518 03205 doi:10.1088/1757-899X/518/3/032056.